

## THE NICMOS POLARIMETRIC CALIBRATION<sup>1</sup>

D. BATCHELDOR,<sup>2</sup> A. ROBINSON,<sup>2</sup> D. AXON,<sup>2</sup> D. C. HINES,<sup>3</sup> W. SPARKS<sup>4</sup> & C. TADHUNTER<sup>5</sup>  
*PASP Accepted*

### ABSTRACT

The value of accurately knowing the absolute calibration of the polarizing elements in the Near Infrared Camera and Multi-Object Spectrometer (NICMOS) becomes especially important when conducting studies which require measuring degrees of polarization of close to 1% in the near infrared. We present a comprehensive study of all previously observed polarimetric standards using the NIC2 camera on NICMOS. Considering both pre- and post-NICMOS Cooling System observations we find variations in the polarimetry consistent with the effects of sub-pixel mis-alignments and the point spread function. We also measure non-zero results from unpolarized standards indicating an instrumental polarization of  $p \approx 1.2\%$ ,  $\theta \approx 88^\circ$ . The lack of polarized and unpolarized standard stars with which to perform a comprehensive calibration study means we cannot be confident that the current calibration will be effective for a number of recent large NICMOS GO programs. Further observations of polarimetric standards are needed in order to fully characterize the behavior of NICMOS at around  $p = 1\%$ .

*Subject headings:* instrumentation: polarimeters, methods: data analysis

### 1. INTRODUCTION

While photometry and spectroscopy provide information on spatial distributions, chemical compositions, and dynamics, polarimetry adds a valuable extra data dimension that can be used to determine the geometry of astronomical objects and the properties of interstellar particles (Antonucci & Miller 1985; Henney, Raga & Axon 1994; Kasen et al. 2003). Polarized light may intrinsically originate from the emission process or it may be induced via interactions with a diffuse medium (Collett 1992; Landi degl’Innocenti 2002). In either case, the preferred orientation of the electromagnetic vector, as well a quantitative measure of that preference, can be determined by placing polarizing elements in the light paths of detectors and deriving the Stokes parameters (Chandrasekhar 1960).

From the ground some care is needed in determining the Stokes parameters as the atmosphere introduces photometric variations with amplitudes similar to those expected from the polarized light. Space based polarimeters are not exposed to these anomalies and can use multiple polarizing filters to gather the required information. However, multichannel polarimeters (Serkowski, Mathewson & Ford 1975), which are yet to be employed on space based polarimeters, do reduce some of the complexities of the data reduction through synchronous recovery of the Stokes parameters. In fact, with enough care, ground-based polarimeters can mea-

sure fractional polarizations of  $10^{-6}$  or less (Hough et al. 2005).

Dust frequently enshrouds many interesting astronomical objects and inhibits the transmission of optical wavelengths. This effect declines as the wavelength of the light increases, thus many studies are carried out in the infrared. It is therefore of great advantage to be able to carry out polarimetric studies with the Near Infrared Camera and Multi-Object Spectrometer (NICMOS) on board the *Hubble Space Telescope (HST)*.

As with many instruments, NICMOS executes programs that cover a wide range of required accuracies and sensitivities. It is therefore essential to probe the polarimetric capabilities of NICMOS, especially in low polarization targets, and assess any signatures that may be introduced by the instrument itself. We present here such an assessment based on the previous efforts of, for example, Hines, Schmidt & Schneider (2000) and Hines (2002). By examining the on-line data archive for NICMOS we can directly compare the results from polarimetric standards whose degree and orientation of polarization have been determined during other investigations. The study is limited to include data obtained with the NIC2 ( $\Delta\lambda = 1.9 - 2.1\mu\text{m}$ ) camera as the number of previous NIC1 ( $\Delta\lambda = 0.8 - 1.3\mu\text{m}$ ) studies, excluding the calibration data, is low. In addition, these NIC1 programs generally probe polarizations of  $\sim 40\%$ , i.e., #7264, where high accuracies are not necessarily needed. However, future works similar to those carried out here may also be prudent for NIC1.

In § 2 we describe the data and its subsequent reduction. The methods used in determining the degree and orientation of polarization are outlined in § 3. The results are presented in § 4 before being discussed and concluded in § 5 and § 6 respectively.

### 2. OBSERVATIONS AND DATA REDUCTION

During the *HST* second servicing mission in 1997, the Faint Object Spectrograph was replaced by NICMOS. This instrument operates from  $0.8 - 2.5\mu\text{m}$  using

arXiv:astro-ph/0601541v1 24 Jan 2006

<sup>1</sup> Based on observations made with the NASA/ESA Hubble Space Telescope obtained at the Space Telescope Science Institute, which is operated by the Association of Universities for Research in Astronomy, Incorporated, under NASA contract NAS 5-26555.

<sup>2</sup> Department of Physics, Rochester Institute of Technology, 84 Lomb Memorial Drive, Rochester, NY, 14623, USA. email: dpbpci@astro.rit.edu

<sup>3</sup> Space Science Institute, 4750 Walnut Street, Suite 205, Boulder, CO 80301, USA

<sup>4</sup> Space Telescope Science Institute, 3700 San Martin Drive, Baltimore, MD, 21218, USA

<sup>5</sup> Department of Physics & Astronomy, University of Sheffield, Sheffield, S3 7RH, UK

TABLE 1  
DETAILS OF OBSERVATIONS

Target	Type	RA (J2000)	Dec (J2000)	Epoch	Orientation ( $^{\circ}$ )	PID
CHA-DC-F7	B5V (Pol.)	10 56 12.91	-76 35 54.2	1997-09-13	-36.48	7692
		10 56 12.03	-76 35 52.0	1998-04-20	-179.00	7958
		10 56 12.03	-76 35 52.0	1998-07-05	-106.49	7692
		10 56 12.13	-76 35 53.2	2002-09-02	-50.83	9644
		10 56 12.15	-76 35 53.3	2003-05-20	-160.83	9644
G191B2B	DAw (Unpol.)	05 05 30.80	+52 49 52.9	1997-12-24	-74.32	7904
HD64299	A1V (Unpol.)	07 52 25.61	-23 17 50.3	1997-09-01	12.71	7692
HD283812	A2V (Pol.)	04 44 25.16	+25 31 43.1	1997-09-28	14.52	7692
		04 44 25.16	+25 31 42.4	1997-12-04	-47.48	7692
HD331891	A4III (Unpol.)	20 12 2.29	+32 47 45.2	1997-09-01	-93.57	7692
		20 12 2.08	+32 47 42.2	1998-04-26	32.55	7958
		20 12 2.11	+32 47 43.5	2002-09-09	-109.63	9644
		20 12 2.11	+32 47 43.5	2003-06-08	0.57	9644

NOTE. — Types taken from SIMBAD (<http://simbad.u-strasbg.fr/Simbad>), all other data are as they appear in the *HST* archive (<http://archive.stsci.edu/hst/>). (Pol.) and (Unpol.) after the stellar type refers to polarized and unpolarized standards respectively.

three independent cameras. The setup allows for broad, medium and narrow band imaging, coronagraphic imaging, broad-band imaging polarimetry, and grism spectroscopy. NIC2, the camera focused on in this study, is a  $256 \times 256$  HgCdTe array with a  $0''.075$  pixel scale giving a  $19''.2 \times 19''.3$  field of view (Thompson et al. 1998). After installation on *HST* the dewar was allowed to be brought up to operating temperature. Unfortunately, this temperature was not tested on the ground and the subsequent ice expansion provided enough dewar deformation to allow contact between one of the optical baffles and the vapor cooled shield. The resulting heat sink not only altered the foci of the three cameras, but also depleted the cryogen by the beginning of 1999 (two and a half years ahead of schedule). However, a mechanical cryocooler, the NICMOS Cooling System (NCS), which was successfully installed in March 2002, has since brought NICMOS back to life and restored the infrared capabilities of *HST*. While the instrument performance is comparable pre- and post-NCS (Hines 2002), it must be noted that NICMOS now displays a different set of characteristics. The reason for these changes are at present unclear, however, for individual observations, these effects can be incorporated as changes in the transmission efficiencies of polarizing elements. One must also be aware that different quadrants of the array may exhibit different bias levels introduced by resetting the array, plus additional bias offsets that are related to operating temperature and main bus voltage (Bergeron 2005). While this “pedestal effect” has been reduced by modified flight software, it has not been entirely eliminated and may lead to inconsistent polarization measurements. More specific details can be obtained from the NICMOS Instrument Handbook (Schultz et al. 2005).

A comprehensive search of the NICMOS data archive has been performed with the aim of analyzing all observed polarimetric standard stars. There are also a number of extended sources (e.g. CRL 2688 - the Egg Nebula) available for use in a calibration study. However, the ground truth for such objects is useless as the measured polarizations are dependent on resolution. They also generally exhibit a high degree of polarization and are of

ten variable. Consequently, such objects will not be conducive to determining the polarimetric accuracies for the low polarization targets ( $\lesssim 5\%$ ) with which we are concerned. A prerequisite for the standards to be included in the sample is independent polarization measures from well calibrated and characterized polarimeters. The polarimetric standards found, and associated details, are presented in Table 1. In addition to the data in Table 1 there are also pre-NCS data for two unpolarized standards, HD10700 and HD30652 (Leroy & Le Borgne 1989; Leroy 1993). Unfortunately, the program for which these observations were made (#7614) called for the investigation of circumstellar structures. The actual stars are therefore hopelessly overexposed for accurate study here.

The data and calibration files were retrieved and passed through the latest versions of the *calnica* and *calnicb* pipelines where appropriate. Each non-destructive readout of individual observations was examined. The total counts in each *multiaccum* frame were inspected as a function of the total exposure time. Deviations of this curve of growth from linear, especially at very early times, were deemed to be evidence for the existence of signal persistence. In the cases where the telescope was offset between exposures, the areas of the array exposed to source photons in the previous visit were also examined for persistence. The individual exposures were also checked for any remaining cosmic rays or hot pixels not flagged by the reduction routine.

The *apphot* package in IRAF<sup>6</sup> was used in order to perform aperture photometry on each polarized standard. Circular apertures with radii from 0.5 to 50.5 pixels (in 1 pixel intervals) were centroided on each standard. The observable point spread function (PSF) was comfortably included in the outer aperture. In each frame the sky was sampled (and removed from the target photometry) using a disk whose inner annulus was defined by the edge of the observable PSF, and whose outer annulus was de-

<sup>6</sup> IRAF is distributed by the National Optical Astronomy Observatories, which are operated by the Association of Universities for Research in Astronomy, Inc., under co-operative agreement with the National Science foundation.

fined by the edge of the array. In every case the sky aperture was large enough to avoid the irregularities introduced by the small number statistics associated with Poisson noise.

### 3. DETERMINING P AND THETA

The methodologies behind extracting the degree and orientation of polarization have been specifically addressed for NICMOS by many authors (Mazzuca, Sparks & Axon 1998; Mazzuca & Hines 1999; Sparks & Axon 1999; Hines, Schmidt & Schneider 2000; Hines 2002). However, we briefly revisit the linear technique for the case of three non-ideal polarizers here.

The reduced, sky subtracted, instrumental counts (in  $\text{DN s}^{-1}$  space) through each polarizing element are used to define an observed intensity vector of the form  $a = [I_1, I_2, I_3]$ . The degree and orientation of polarization ( $p$  and  $\theta$ ) are defined by the Stokes parameters which also define a vector of the form  $b = (I, Q, U)$ . The two vectors  $a$  and  $b$  are simply related to each other by the linear expression  $[C]b = a$ , where  $[C]$  is a matrix describing the characteristics of the  $k^{\text{th}}$  polarizer, namely the polarizer efficiency ( $\eta_k$ ), the actual orientation (in radians) of the polarizer ( $\phi_k$ ), the fraction of the light transmitted in the parallel direction ( $t_k$ ), and the fraction of light transmitted in the perpendicular direction ( $l_k$ ). The transmission coefficients are then described by;

$$X_k = \frac{1}{2}t_k(1 + l_k) \quad (1)$$

$$Y_k = X_k(\cos 2\phi_k) \quad (2)$$

$$Z_k = X_k(\sin 2\phi_k) \quad (3)$$

allowing the matrix  $[C]$  to be defined as follows:

$$C = \begin{bmatrix} X_1 & \eta_1 Y_1 & \eta_1 Z_1 \\ X_2 & \eta_2 Y_2 & \eta_2 Z_2 \\ X_3 & \eta_3 Y_3 & \eta_3 Z_3 \end{bmatrix} \quad (4)$$

The linear expression  $[C]b = a$  can then be solved for  $I, Q$  and  $U$  using, for example, LU decomposition. We can then solve for  $p$  and  $\theta$  using Equations 5 and 6.

$$p = 100\% \times \frac{\sqrt{Q^2 + U^2}}{I} \quad (5)$$

$$\theta = \frac{1}{2} \arctan \frac{U}{Q} \quad (6)$$

In Equation 6 a  $360^\circ$  arctangent function is assumed. In addition, the orientation of the frame has to be subtracted from  $\theta$  in order to retrieve the on sky position angle.

We have coded the above process in IDL in order to solve for  $p$  and  $\theta$  given three lists of apertures and photometric data. This process has also been coded by Mazzuca & Hines (1999) into the IDL routine *polarize.pro*.<sup>7</sup> Their routine takes the three polarized images and produces two dimensional maps of  $p$  and  $\theta$ , whereas the code used here produces the measured polarization through defined apertures. The two methods are precisely consistent when tested on flat (polarized) data,

<sup>7</sup> [http://www.stsci.edu/hst/nicmos/tools/polarize\\_tools.html](http://www.stsci.edu/hst/nicmos/tools/polarize_tools.html)

TABLE 2  
POLARIMETRIC CALIBRATION PARAMETERS

Filter	$\theta_k$ ( $^\circ$ )	$\eta_k$	$l_k$	$t_k$	
				-NCS	+NCS
POL0L	8.84	0.7313	0.1552	0.8981	0.8779
POL120L	131.42	0.6288	0.2279	0.8551	0.8379
POL240L	248.18	0.8738	0.0673	0.9667	0.9667

NOTE. — “-” and “+” refer to pre- and post-NCS coefficients respectively.

i.e., one value of  $I$  for each polarizer across the entire array.

In addition to the aforementioned process, we have also included an estimation of the errors associated with  $p$  and  $\theta$  introduced by the variance in the count rate. The estimation is taken from Sparks & Axon (1999) and is defined by the variance and covariance in the  $(Q, U)$ -plane.

#### 3.1. The Polarimetric Calibration Parameters

The first estimates of the polarimetric calibration parameters were presented by Hines, Schmidt & Lytle (1997). Preflight thermal vacuum tests of the polarizing optics found each element to have a unique polarizing efficiency and position angle offset. The values of  $\phi_k, \eta_k, l_k$  and  $t_k$  were estimated by attaching a polarizer to the Calibrated InfraRed source (CIRCE). This provided uniform illumination across the entire array at a known position angle and magnitude. Following the on orbit observations of the polarized standard CHA-DC-F7 and the unpolarized standard HD331891, values for  $t_k$  were adjusted based on exposures from two separate roll angles and from two separate epochs (Hines 1998; Hines, Schmidt & Schneider 2000). Using the pre-NCS coefficients from Table 2, values of  $p$  for CHA-DC-F7 were found to be within  $\sim 0.2\%$  of the ground based values. Post-NCS the values of  $t_k$  were again adjusted (0.8774, 0.8381, 0.9667; Hines 2002) and used in such studies as Ueta, Murakawa & Meixner (2005). The coefficient matrix used in this study has been constructed from the parameters in Table 2 using the latest revised values of  $t_k$  (Hines 2005).

#### 3.2. Testing the Routine

The IDL routine was extensively tested in order to check its performance against known (simulated) polarizations. The testing also provided examples of how the instrument itself may affect the observed polarization (e.g., noise and the PSF). We have generated data, mapped onto the NICMOS pixel grid, which simulates a star with a Gaussian surface brightness profile (both with and without the effects of Poisson noise), a point source with a TinyTim PSF (Krist & Hook 2004), and the effects of sub-pixel shifts between the pointing of the three polarizers. Small spatial shifts between polarizing elements are not unexpected and may allow flux gathered in one frame to fall into an inter-pixel gap in another.

The resulting polarization profiles (which all use the post-NCS transmission coefficients for NIC2), i.e., the polarization as measured through progressively larger

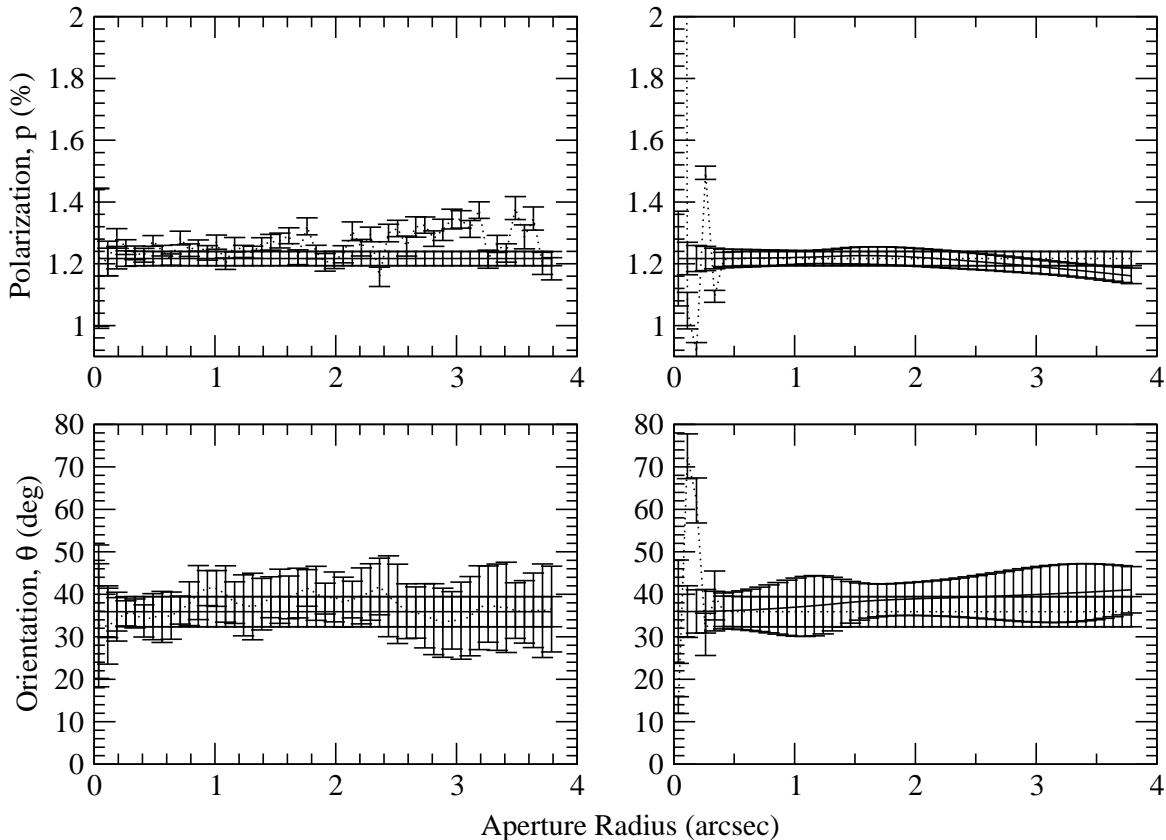


FIG. 1.— Results from testing the polarimetry routine. (*Left column*) From a Gaussian surface brightness profile with (dotted line) and without (solid line) Poisson noise. (*Right column*) Using the PSFs as generated by `TinyTim`. The solid lines are for perfectly aligned frames whereas the dotted lines show the effects of sub-pixel mis-alignment using a Gaussian profile.

apertures, are presented in Figure 1. It can be seen that the routine behaves as one would predict. Generally there are variations plus larger errors on the small scale, and constant results for large apertures. The addition of the `TinyTim` PSF is seen to increase the small scale variations and errors. Introducing sub-pixel shifts allows the small scale variations to grow. In all noiseless cases the profile behavior is stable in apertures larger than  $0''.5$ . The best polarization estimates for real data are therefore likely to come from large apertures enclosing most of the flux.

In all cases, to get appropriate estimates for the effects of Poisson noise, we have replicated the signal to noise ratios typically seen in the standards ( $\sim 50$ ) as well as the expected polarizations ( $\sim 1.2\%$ ).

#### 4. RESULTS

We now pay close attention to each of the targets listed in Table 1. The results and details of previous ground based polarimetry observations, as well as the archived NICMOS results, are presented individually, summarized in Table 3 and compared in Figure 3.

In order to correct for the wavelength dependence of polarization (Serkowski, Mathewson & Ford 1975) and allow a comparison between these NICMOS measurements and ground based results, one can use the “Serkowski curve” (Serkowski 1973; Wilking, Lebofsky & Rieke 1982) to find  $p(2.05)$ . This notation corresponds to the value of  $p$  (%) at the  $2.05\mu\text{m}$  wavelength of NIC2. However, in both cases where

this may be necessary, there are direct measurements at  $p(2.04)$  by Whittet et al. (1992).

We have considered photometry from data which have also had the model PSFs, as generated by `TinyTim`, removed using the Lucy-Richardson deconvolution. In the test cases (CHA-DC-F7 and HD331891) a change of less than  $0.1\%$  in  $p$  was seen inside the PSF. Using large apertures there was no difference as all of the flux was enclosed without the need for deconvolution. However, the advantage of de-convolving the PSF comes when attempting to visually identify remaining hot pixels and cosmic rays. The extra flux that may be introduced by such pixels hiding in the artifacts of the PSF will have a detrimental effect on the photometry and therefore the measured polarization. The residuals between the PSF deconvolved frame and frame containing the PSF were therefore carefully examined for further evidence of hot pixels and cosmic rays. Two dimensional interpolation is used to replace any such features. All of the remaining polarimetry was carried out with PSF deconvolution.

In this study, where we can see the polarimetric behavior with radius, it is not obvious which aperture will be consistent with previous studies; photometric aperture sizes have not been published. Here we choose to inspect each frame in order to report the measured polarization in an aperture that includes all of the observed flux distributed across the array by the PSF. The aperture size is also reported in Table 3.

TABLE 3  
RESULTS OF THIS AND PREVIOUS STUDIES

Target	Previous				This Study			
	$p_{pre}(\%)$	$\theta_{pre}(\circ)$	$p(\lambda_{max})(\%)$	Ref.	Epoch	R(")	$p(\%)$	$\theta(\circ)$
CHA-DC-F7	$1.19 \pm 0.01$	$126 \pm 4$	5.98	1	1997-09-13	0.34	$0.94 \pm 0.03$	$116 \pm 7$
					1998-04-20	0.34	$2.22 \pm 0.03$	$86 \pm 4$
					1998-07-05	0.34	$0.95 \pm 0.03$	$116 \pm 2$
					2002-09-02	0.34	$1.05 \pm 0.02$	$119 \pm 5$
					2003-05-20	0.34	$1.19 \pm 0.03$	$111 \pm 4$
G191B2B	$0.09 \pm 0.05$	$157 \pm 1$	n/a	2,3	1997-12-24	0.26	$1.2 \pm 0.4$	$90 \pm 5$
HD64299	$0.15 \pm 0.03$	...	n/a	2	1997-09-01	0.34	$1.46 \pm 0.06$	$67 \pm 4$
HD283812	$1.31 \pm 0.07$	$35 \pm 2$	6.29	1	1997-09-28	0.79	$3.11 \pm 0.08$	$121 \pm 3$
					1997-12-04	0.79	$1.40 \pm 0.03$	$35 \pm 4$
HD331891	$0.04 \pm 0.03$	$79 \pm 1$	n/a	2,3	1997-09-01	0.34	$1.32 \pm 0.02$	$106 \pm 4$
					1998-04-26	0.34	$1.19 \pm 0.02$	$97 \pm 5$
					2002-09-09	0.34	$1.41 \pm 0.02$	$90 \pm 3$
					2003-06-08	0.34	$0.77 \pm 0.02$	$79 \pm 3$

NOTE. — References: 1. Whittet et al. (1992). 2. Turnshek et al. (1990). 3. Schmidt, Elston & Lupie (1992). The values of  $p_{pre}$  and  $\theta_{pre}$  are those taken from the literature *after* the  $p(\lambda_{max})$  correction. R(") refers to the aperture radius through which the observation was made.

#### 4.1. CHA-DC-F7

The polarimetric properties of CHA-DC-F7 were originally reported by Whittet et al. (1992) before being used in the previous NICMOS polarimetry studies of Hines, Schmidt & Lytle (1997), Hines (1998), Hines, Schmidt & Schneider (2000) and Hines (2002). Whittet et al. (1992) report, from ground based measurements,  $p(\lambda_{max}) = 5.98\%$  at  $0.55\mu\text{m}$  with an instrumental polarization of  $0.03\%$ , and  $p(2.04) = 1.19\% \pm 0.01\%$  at  $\theta = 126^\circ \pm 4^\circ$  which we use in this comparison. The NICMOS polarimetry studies (Hines, Schmidt & Schneider 2000) report  $p(2.05) = 0.97\% \pm 0.2\%$  at  $\theta = 119^\circ \pm 6^\circ$  and  $p(2.05) = 1.00\% \pm 0.2\%$  at  $\theta = 119^\circ \pm 6^\circ$  for the 1997 and 1998 epochs respectively.

Exposures of 13.95 seconds were made, at every epoch, through each of the three polarizing elements. With the exception of the 1997 and July 1998 epochs all observations used a four point dither pattern, each frame being offset by  $2/3$ . All data in this study are consistent with previous polarization estimates apart from the April 1998 epoch. We note that of all the data for CHA-DC-F7 these observations are closest ( $\sim 50$  minutes) to a South Atlantic Anomaly passage and are the only pre-NCS observation to be dithered. While the number of cosmic ray hits does not appear to be higher than in the other epochs, we have noticed large differences in the photometry from different parts of the array. Figure 3 demonstrates the difference between photometry obtained from the individual non-destructive readouts from the dithered and non-dithered data. It can be seen that there is a larger spread in the photometry from the dithered data, which in turn could lead to a greater amount of polarization due to the greater flux differences between the polarizers. This effect is not present in post-NCS observations and suggests that the pedestal effect is non-negligible in pre-NCS dithered polarimetry. It is well known that the NCS produces much more stable temperatures for the array (Schultz, Roye & Sosey 2003; Arribas et al. 2005), which is why the pedestal effects are much less dramatic than when NICMOS was cooled with

nitrogen ice. We also note that there are late variations from linear ( $\sim 10$  seconds onward) in the photometric curves of growth. This may be indicative of saturation, or at least non-linearity, but we do not find any evidence for this in the Data Quality (DQ) data extensions. DQ values of 3072 are reported which correspond to ‘‘Pixel containing source’’ (1024) and ‘‘Pixel has signal in the 0th read’’ (2048), not ‘‘Saturated pixel’’ (64) or ‘‘Poor or uncertain Linearity correction’’ (2)<sup>8</sup>. Following on from this we also do not see any non-linearity early in the curves of growth. This indicates that persistence is insignificant.

#### 4.2. G191B2B

Schmidt, Elston & Lupie (1992) report G191B2B to be an unpolarized standard with  $p(0.55) = 0.09\% \pm 0.05\%$  and  $\theta = 157^\circ$  from observations using the ‘‘Two-Holer’’ polarimeter. The instrumental polarization is estimated to be 0.05-0.10%.

Each NICMOS observation has an exposure time of 23.97s and has been dithered using a three point pattern. Compared to the CHA-DC-F7 observations the point spacings for these dithers are small. In addition, the spread in the photometric curves of growth is less than those seen in Figure 3. Nevertheless the results from this study do show polarization at a level of 1.2% where something much closer to zero is expected.

#### 4.3. HD64299

HD64299 is listed as an unpolarized standard ( $p(\sim 0.55) = 0.15\% \pm 0.03\%$ ) by Turnshek et al. (1990). Ageorges & Walsh (1999) also use this standard in order to characterize the instrumental polarization of the ADONIS polarimeter ( $p_{ins}(\sim 2.0) \approx 1.5\%$ ).

No dithering was used during each of the 11.96s exposures and there is no evidence for persistence or saturation. However, as with the case of G191B2B, we measure a polarization that is inconsistent with zero.

<sup>8</sup> See Chapter 2 of the NICMOS Data Handbook, Mobasher & Roye (2004).

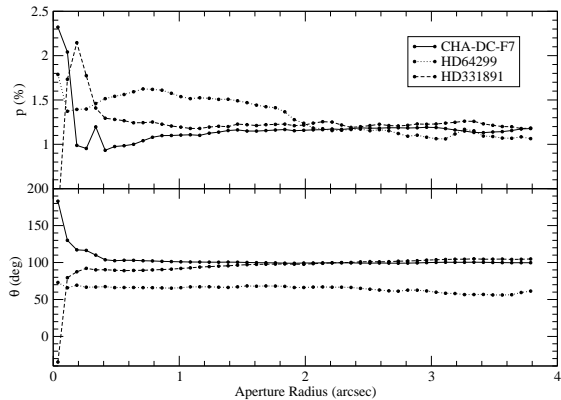


FIG. 2.— Example polarimetric curves of growth. Error bars have been omitted for clarity but are approximately  $\pm 0.03\%$  in  $p$  and  $\pm 4^\circ$  in  $\theta$ .

#### 4.4. HD283812

The polarized properties of HD283812 have been reported to be  $p(\sim 0.55) = 4\% \pm 1\%$ ,  $\theta = 33.8^\circ$  and  $p(0.55) = 6.29\% \pm 0.05\%$ ,  $\theta = 32^\circ \pm 1^\circ$  by Turnshek et al. (1990) and Whittet et al. (1992) respectively. Whittet et al. (1992) also measures  $p(2.04) = 1.31\% \pm 0.07\%$  at  $\theta = 35^\circ \pm 2^\circ$ . As HD283812 is an extended source, we use the brightest northern component to begin the centroid for photometry.

Both epochs of the data for HD283812 had exposure times of 5.98s. Dithering was only applied to the September 1997 epoch data however, where the point spacing was large ( $5''.0$ ). The dithered photometric curves of growth show a spread comparable to the dithered data in Figure 3, there is no evidence of persistence. We find that the dithered data shows a larger degree and orientation of polarization than expected but the non-dithered data is entirely consistent.

#### 4.5. HD331891

Turnshek et al. (1990) and Schmidt, Elston & Lupie (1992) report HD331891 (BD32+3739) to be an unpolarized standard with  $p(\sim 0.43) = 0.04\% \pm 0.03\%$ . This standard was also used in determining the pre- and post-NCS coefficients.

Whereas all exposures were 5.98s, all but the 1997 data have been dithered with a  $2''.3$  four point spacing. There is no evidence of persistence and none of the data shows an exaggerated spread in the photometric curves of growth. Nevertheless, all epochs show non-zero degrees and orientations of polarization. These results are consistent with the findings of Ueta, Murakawa & Meixner (2005) who use the same data with the same coefficients to find  $p(2.05) = 1.4\%$ . They attribute the  $\gtrsim 1\%$  polarization, i.e., greater than the  $\lesssim 1\%$  instrumental polarization reported by Hines, Schmidt & Schneider (2000), to “systematics in the data reduction procedure.” However, the estimate of  $p_{ins} \lesssim 1\%$  was based upon ground based-thermal vacuum tests and not from on-orbit data.

### 5. DISCUSSIONS

As demonstrated by Figure 2 we can see that the simulated (Figure 1) and real data compare well. In all cases

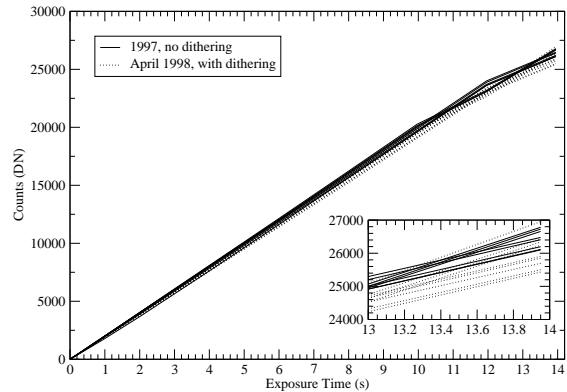


FIG. 3.— Comparing non-destructive readouts from dithered and un-dithered data for CHA-DC-F7. Inset: An expanded view from the end of the exposures highlighting the photometric differences.

the large-scale values of  $p$  and  $\theta$  are clearly stable. The inner variations due to the residual PSF and sub-pixel mis-alignment are also seen, but are insignificant outside of a radius which approximately corresponds to the first airy ring of the PSF ( $\sim 0''.3$ ), i.e., as long as the photometric apertures contain all of the flux spread by the PSF, consistent values of  $p$  and  $\theta$  will be measured.

It is clear that there are significant differences in polarizations measured at separate epochs for CHA-DC-F7 and HD283812. It is unlikely that these variations are intrinsic to the objects. In both cases it is noted that the data are pre-NCS and dithered. It is also unclear why such an anomaly is not seen in the pre-NCS dithered data for HD331891. However, as suggested in §4.1, this may be an artifact from the pedestal effect. There do exist several IRAF software packages to remove the pedestal effect (*pedsky*, *pedsub*), but as the dither allows a check of the NICMOS polarization properties in each quadrant, we can check to see if this is the reason for the discrepant results by performing our routine only on the data from a single pointing. Accordingly we have re-reduced the raw data files through the *calnica* pipeline and determined the polarization results from each quadrant. The results are presented in Table 4. It can be seen that the individual pointings give polarization measures consistent with un-dithered data, and that the pre-NCS pedestal effect can induce variations of  $\Delta p \approx 0.2\%$  and  $\Delta \theta \approx 15^\circ$  between different quadrants. Post-NCS the pedestal effect does not appear to have affected the results, however, it is clear that the pedestal effect does produce slightly different polarizations in each quadrant of the array.

We have measured polarization in all of the targets which have previously been listed as unpolarized. Such findings suggest that there may be a low level of instrumental polarization. From Table 3 it can be seen that, on average, this instrumental polarization has a magnitude  $p \approx 1.2\%$  at a positional angle of  $\theta \approx 88^\circ$ . We now demonstrate how such an instrumental polarization may be corrected for.

The fact that polarized standards have been measured to be consistent with previous studies (CHA-DC-F7, HD283812) allows us to be confident that the results for the unpolarized standards are real, and that

TABLE 4  
PRE-NCS PEDESTAL CHECK

Quadrant	CHA-DC-F7		HD283812	
	$p(\%)$	$\theta(^{\circ})$	$p(\%)$	$\theta(^{\circ})$
1	$1.25 \pm 0.03$	$115 \pm 6$	$1.49 \pm 0.03$	$31 \pm 2$
2	$1.12 \pm 0.03$	$128 \pm 7$	$1.41 \pm 0.01$	$24 \pm 4$
3	$1.13 \pm 0.03$	$113 \pm 7$	$1.53 \pm 0.03$	$35 \pm 4$
4	$1.21 \pm 0.02$	$114 \pm 6$	$1.31 \pm 0.03$	$36 \pm 2$

we may be seeing a residual instrumental polarization. The low number of observed unpolarized standards and the pedestal effect make it difficult to be confident in the exact nature of the instrumental polarization, but we can nevertheless make an attempt to correct the data for this. As the degree and orientation of polarization are derived in Stokes ( $I, Q, U$ ) space this is also where we can perform an instrumental correction. It is essential that the correction is carried out in the ( $Q, U$ )-plane for each standard and not in the celestial coordinate system. The unpolarized standard data from pre- and post-NCS observations are considered separately. While the ( $Q, U$ ) quadrants are consistent between the polarized standards, the actual values of  $Q$  and  $U$  are dependent on  $I$ . The corrections are therefore averaged (weighted by the errors in  $Q$  and  $U$ ) across all observed standards after being normalized by the intensity, rather than being simply carried out in the ( $Q, U$ )-plane. The results from the correction are presented in Table 5. It can be seen that the dispersion around the expected and previously reported results has been reduced. The  $\chi^2$  for the polarized standards about the expected values is now  $\sim 0.01$  as compared to  $\sim 0.1$  without the ( $Q, U$ ) correction.

It is also possible to null the polarization in unpolarized targets by adjusting the on orbit derived transmission coefficients. As  $Q = U = 0$  in unpolarized sources,  $t_k$  can be derived by considering  $I_k = IX_k$  and fixing  $t_3 = 0.9667$ . Solving  $t_1$  and  $t_2$  for  $p = 0\%$  and  $\theta = 0^{\circ}$  in HD331891 across all photometric apertures results in the co-efficient profiles presented in Figure 4. It can be seen in Figure 4 that in the central most aperture the co-efficients derived from the 2002 epoch (dashed line) are consistent with the co-efficients quoted in Table 2. Similar small scale variations to that of the observed polarimetric curves of growth are also seen. Taking an average of the derived 2003 epoch co-efficients, outside of the inner arc-second, and carrying through the photometric errors, gives us  $t_1 = 0.8717 \pm 0.0005$  and  $t_2 = 0.8341 \pm 0.0005$ . Applying these adjusted co-efficients (which are within 1% of the original co-efficients) to the 2003 data for CHA-DC-F7 produces a typical change of  $\delta p \approx 0.1\%$  and  $\delta \theta \approx 3^{\circ}$  over the values of  $p$  and  $\theta$  derived from the original co-efficients.

Adjusting the transmission co-efficients to null the measured polarization in a single unpolarized standard may provide a “quick fix” for some data, but it is by no means a concrete solution to the underlying problem. After all, it is possible there have been no changes in the transmission co-efficients. Ideally we would be able to characterize these effects by observing several polarized

TABLE 5  
CORRECTING FOR INSTRUMENTAL POLARIZATION

Target	Epoch	$p_{corr}(\%)$	$\theta_{corr}(^{\circ})$	
CHA-DC-F7	1997-09-13	$1.24 \pm 0.03$	$128 \pm 7$	
	1998-04-20	$1.25 \pm 0.03^*$	$117 \pm 5$	
	1998-07-05	$1.21 \pm 0.04$	$133 \pm 5$	
	2002-09-02	$1.21 \pm 0.03$	$109 \pm 7$	
	2003-05-20	$1.12 \pm 0.04$	$124 \pm 6$	
G191B2B	1997-12-24	$0.4 \pm 0.9$	$-7 \pm 19$	
	HD64299	1997-09-01	$0.34 \pm 0.05$	$-5 \pm 17$
	HD283812	1997-09-28	$1.32 \pm 0.04^*$	$33 \pm 7$
HD331891	1997-12-04	$1.38 \pm 0.09$	$29 \pm 5$	
	1997-09-01	$0.36 \pm 0.05$	$6 \pm 11$	
	1998-04-26	$0.33 \pm 0.04$	$5 \pm 13$	
	2002-09-09	$0.26 \pm 0.04$	$-2 \pm 11$	
	2003-06-08	$0.26 \pm 0.03$	$2 \pm 15$	

NOTE. — Epochs marked with “\*” are the results from the 1st quadrant of NIC2 only.

standards at the cardinal angles of the polarizers (this greatly reduces the degrees of freedom in the coefficient matrix). This would also allow us to see if there is an instrumental polarization that is dependent on the orientation and level of polarization in the object as well as the roll angle of *HST*. For example, it is possible that the sensitivity of the mirrors to polarized light is producing some reflective retardance. Unfortunately, there is, at present, insufficient calibration data available in the archive with which to fully check this possibility. There does exist data for two polarized objects, CHA-DC-F7 and HD283812, at multiple roll angles (see Table 1), but this statistically insignificant sample inhibits us from drawing any conclusions about the nature of an observationally dependent instrumental polarization.

While previous polarimetric studies with NICMOS have not needed to be concerned with such characteristics due to the high levels of observed polarization (Ueta, Murakawa & Meixner 2005), as the capabilities of NICMOS are stretched by more and more ambitious programs so will the need to accurately measure low levels of polarization. In fact, a number of programs needing these levels of accuracy have already been executed. For example, #10160 (The nuclear scattering geometry of Seyfert galaxies) and #10410 (Anisotropy and obscuration in the near nuclear regions of powerful radio galaxies) will both require high accuracies as AGN generally display  $p \approx 1 - 5\%$ . In addition, as the James Webb Space Telescope will not be flying with polarimetry optics, NICMOS will remain the only instrument capable of performing such high precision imaging polarimetry on faint objects.

The recent polarization calibration for the Advanced Camera for Surveys (Biretta et al. 2004; Biretta & Kozhurina-Platais 2004; Kozhurina-Platais & Biretta 2004, 2005) presents an example for the NICMOS calibration. In order for the aforementioned programs to be successful, new data on a number of both polarized standards, at various degrees and orientations of polarization, and unpolarized standards should be obtained. Pointings should be gridded across the detector in order to investigate field dependence. A number of exposures, in each polarizer,

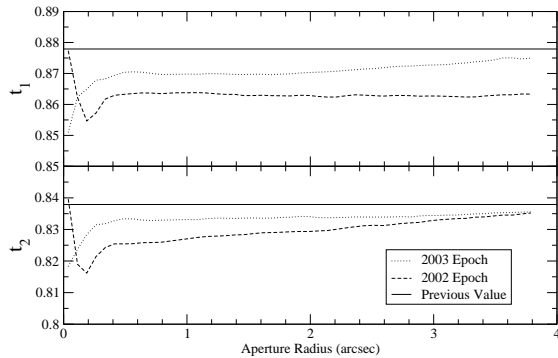


FIG. 4.— The values of  $t_k$  required to null the unpolarized standard HD331891. The value of  $t_3$  is held constant at 0.9667.

at different roll angles should also be employed in order to replicate the ground characterization. This will allow the derivation of element independent transmission co-efficients (from point sources) and will allow tests for higher order calibration effects. Such thorough observations may also shed some light as to the reason for the change in behavior from Cycles 7 and 11.

## 6. CONCLUSIONS

We have conducted polarimetric analyses on all (un)polarized standards available in the NICMOS data archive for the NIC2 camera. The principle aim was to determine the behavior of the instrument at low levels of polarization. We have thoroughly tested our routine for deriving aperture polarimetry of objects and found it to be robust. It has also demonstrated that observed small radius variation in the polarimetric curves of growth can be attributed to the effects of sub-pixel mis-alignments between polarizing elements and the point spread function. We have found no evidence for persistence.

Our findings also indicate that there is a measured polarization of  $p \approx 1.2\%$  in unpolarized targets which may indicate an intrinsic instrumental polarization and the need for further tweaking of the on-orbit transmission co-efficients. Assuming we are detecting an instrumental effect we have corrected data for polarized targets in the  $(Q, U)$ -plane and found the dispersion around previous (ground based) polarization estimates to have been reduced, but not totally removed. We have also derived averaged values of  $t_k$  that null the unpolarized standard HD331891 across all apertures, and found  $t_1$  and  $t_2$  to be 0.8717 and 0.8341, respectively, when fixing  $t_3 = 0.9667$ . In addition, we have attempted to investigate the possibility of an observationally dependent instrumental polarization, but are inhibited from any conclusions by an insignificant sample.

While such levels of residual intrinsic polarization may not hamper studies of highly polarized targets, these levels will have a detrimental effect on studies attempting to measure  $p < 5\%$ . It is clear that a more comprehensive calibration study of NICMOS is critical in order for a number of *HST* programs to be carried out successfully. The current post-NCS calibration archive (one polarized and one unpolarized standard) is insufficient for this to occur effectively. An array of polarized and unpolarized standards should be observed, at many roll angles and in all quadrants of the instrument, in order for the low level polarization characteristics of NICMOS to be properly and fully investigated, understood and removed.

We would like to thank the referee for his careful and thorough reading of this manuscript. His input has greatly improved the paper. Thanks are also extended to Glenn Schneider for his useful comments. Support for this study was provided by NASA through a grant from the Space Telescope Science Institute, which is operated by the Association of Universities for Research in Astronomy, Incorporated, under NASA contract NAS5-26555.

## REFERENCES

- Ageorges, N., & Walsh, J. R. 1999, *A&AS*, 138, 163  
 Antonucci, R. R. J., & Miller, J. S. 1985, *ApJ*, 297, 621  
 Arribas, S. et al. 2005, *ISR NICMOS 2005-005*  
 Bergeron, L. 2006, *The 2005 HST Calibration Workshop*, in prep.  
 Biretta, J., Kozhurina-Platais, V., Boffi, F., Sparks, W., & Walsh, J. 2004, *ISR-ACS 2004-09*  
 Biretta, J. & Kozhurina-Platais, V. 2004, *ISR-ACS 2004-10*  
 Kozhurina-Platais, V. & Biretta, J. 2004, *ISR-ACS 2004-11*  
 Kozhurina-Platais, V. & Biretta, J. 2005, *ISR-ACS 2005-10*  
 Chandrasekhar, S. 1960, *Radiative Transfer*. New York: Dover, pp. 25-37  
 Collett, E. 1992, *Optical Engineering*, New York: Dekker  
 Henney, W. J., Raga, A. C., & Axon, D. J. 1994, *ApJ*, 427, 305  
 Hines, D. C., Schmidt, G. D., & Lytle, D. 1997, *The 1997 HST Calibration Workshop with a New Generation of Instruments*, p. 217, 217  
 Hines, D. C. 1998, *NICMOS and the VLT*, ESO Conference and Workshop Proceedings 55, Wolfram Freudling and Richard Hook eds., p. 63, 63  
 Hines, D. C., Schmidt, G. D., & Schneider, G. 2000, *PASP* 112, 983  
 Hines, D. C. 2002, *The 2002 HST Calibration Workshop*, Edited by Santiago Arribas, Anton Koekemoer, and Brad Whitmore. Baltimore, MD: Space Telescope Science Institute, 2002., p.260, 260  
 Hines, D. C. 2005, *The 2005 HST Calibration Workshop*, in prep.  
 Hough, J., Lucas, P., Bailey, J., Hirst, E., Tamura, M., & Harrison, D. 2005, *The Newsletter of the Isaac Newton Group of Telescopes (ING Newsl.)*, issue no. 9, p. 26-17., 9, 26  
 Kasen, D., et al. 2003, *ApJ*, 593, 788  
 Kirst, J., & Hook, R. 2004, *The Tiny Tim User's Guide*, Version 6.3  
 Landi degl'Innocenti, E. 2002, *Astrophysical Spectropolarimetry*, 1  
 Leroy, J. L., & Le Borgne, J. F. 1989, *A&A*, 223, 336  
 Leroy, J. L. 1993, *A&AS*, 101, 551  
 Mazzuca, L., Sparks, W. B., & Axon, D. J. 1998, *ISR NICMOS 98 017*  
 Mazzuca, L., & Hines, D. C. 1999, *ISR NICMOS 99 004*  
 Mobasher, B. & Roye, E. 2004, *NICMOS Data Handbook*, Diane Karakla, Chief Editor and Susan Rose, Technical Editor, *HST Data Handbook*  
 Schmidt, G. D., Elston, R., & Lupie, O. L. 1992, *AJ*, 104, 1563  
 Schultz, A. B., Roye, E. & Sosey, M. 2003 *ISR NICMOS 2003-003*  
 Schultz, A., et al. 2005, "NICMOS Instrument Handbook", Version 8.0, (Baltimore: STScI)  
 Serkowski, K. 1973, *IAU Symp. 52: Interstellar Dust and Related Topics*, 52, 145  
 Serkowski, K., Mathewson, D. L., & Ford, V. L. 1975, *ApJ*, 196, 261  
 Sparks, W. B., & Axon, D. J. 1999, *PASP*, 111, 1298  
 Thompson, R. I., Rieke, M., Schneider, G., Hines, D. C., & Corbin, M. R. 1998, *ApJ*, 492, L95

- Turnshek, D. A., Bohlin, R. C., Williamson, R. L., Lupie, O. L., Koornneef, J., & Morgan, D. H. 1990, *AJ*, 99, 1243
- Ueta, T., Murakawa, K., & Meixner, M. 2005, *AJ*, 129, 1625
- Whittet, D. C. B., Martin, P. G., Hough, J. H., Rouse, M. F., Bailey, J. A., & Axon, D. J. 1992, *ApJ*, 386, 562
- Wilking, B. A., Lebofsky, M. J., & Rieke, G. H. 1982, *AJ*, 87, 695